

A Fabric-Regulated Soft Robotic Glove with User Intent Detection using EMG and RFID for Hand Assistive Application

Hong Kai. Yap^{1,2#}, *Student Member, IEEE*, Benjamin W. K. Ang^{1#}, Jeong Hoon. Lim³, James C. H. Goh¹, and Chen-Hua Yeow^{*1,4}, *Member, IEEE*

Abstract— This paper presents a soft robotic glove designed to assist individuals with functional grasp pathologies in performing activities of daily living. The glove utilizes soft fabric-regulated pneumatic actuators that are low-profile and require lower pressure than previously developed actuators. They are able to support fingers and thumb motions during hand closure. Upon pressurization, the actuators are able to generate sufficient force to assist in hand closing and grasping during different manipulation tasks. In this work, experiments were conducted to evaluate the performances of the actuators as well as the glove in terms of its kinetic and kinematic assistance on a healthy participant. Additionally, surface electromyography and radio-frequency identification techniques were adopted to detect user intent to activate or deactivate the glove. Lastly, we present preliminary results of a healthy participant performing different manipulation tasks with the soft robotic glove controlled by surface electromyography and radio-frequency identification techniques.

I. INTRODUCTION

Impairment of hand function and mobility is the most common problem that surfaces after developing neurological disorders such as stroke [1], muscular dystrophy [2] and incomplete spinal cord injury [3]. An individual suffering from the impairment will lose the ability to accurately control the hand and digits as well as to perform activities of daily living. In order to restore hand function and mobility, physical therapy and rehabilitation programs comprising repetitive task practice (RTP) are required [4]. However, these procedures are normally labor-intensive and limited to clinical settings. As an alternative to physiotherapist-assisted program, various robotic devices with the ability to assist with repetitive hand movements have been proposed [5].

One class of robotic devices is exoskeletons, which couple to the user through multiple limb segments and

provide movement assistance. However, traditional hand exoskeletons consist of rigid components [6-8] which are normally heavy and constrain the non-actuated degrees of freedom (DOFs) of the joints. This limits the compatibility, comfort and safety levels for the patients. Therefore, these devices are normally restricted in clinical environments and are not suitable for use as an at-home assistive device that can provide assistance for activities of daily living (ADL) and task-specific training. In order to design exoskeletons that are more wearable and lightweight, alternative approaches that utilize compliant materials such as cables [9-11] and soft elastomeric actuators have been adopted. These approaches do not require complicated mechanical setups, which reduce the setup time and the possibility of misalignment. Soft elastomeric actuators have drawn increasing research interest due to their high compliance and low inherent stiffness [12, 13]. They are highly customizable and able to achieve multiple DOFs with a single input (e.g. fluid pressurization). Several research groups have developed wearable soft exoskeletons by combining soft gloves with soft elastomeric actuators [14-17]. These devices provide a greater chance of user acceptance due to their compactness, affordability and customizability [18, 19].

Several pioneer works on soft robotic glove have been accomplished by Polygerinos *et al.* [14, 15]. They have designed a hydraulically actuated soft robotic glove which utilizes fiber-reinforced elastomeric actuators that can be mechanically programmed to generate complex motion paths that are similar to the kinematics of the human finger and thumb. Recently, they have also explored an open-loop surface electromyography (sEMG) algorithm to control the soft robotic glove for performing task-specific hand exercises based on user intent [20].

In this paper, we present our recent developments in the design of another type of soft robotic glove which utilizes pneumatically actuated soft elastomeric actuators (as presented in [16]). We explore another design technique by investigating the morphology of the actuators as well as different types of textiles in order to mechanically program the actuators to generate motion paths that are able to support full hand range of motion without fiber-reinforcement. With respect to user intent detection, we implemented EMG control strategy combined with radio-frequency identification (RFID). The RFID tags serve as non-physical switches for the activation of different hand gestures such as palmar grasp and pincer grasp. With combined EMG-RFID control strategy, complex EMG classification algorithms are not required. The user can activate different hand gestures with minimum number of sEMG electrodes, which further reduce the complexity of the device.

This work was supported by the Ministry of Education AcRF Tier 2 grant (R-397-000-203-112).

*Corresponding author

#These authors contributed equally to the work.

¹Hong Kai Yap, Benjamin W.K. Ang, James C. H. Goh and C. H. Yeow are with the Department of Biomedical Engineering, National University of Singapore, 117575 Singapore (e-mail: hongkai@u.nus.edu; a0096481@u.nus.edu; biehead@nus.edu.sg; bieych@nus.edu.sg).

²Hong Kai Yap is also with the NUS Graduate School for Integrative Sciences and Engineering.

³Jeong Hoon Lim is with the Department of Medicine, National University Hospital, Yong Loo Lin School of Medicine, National University of Singapore, 119228 Singapore. (e-mail: jeong_hoon_lim@nuhs.edu.sg).

⁴Chen-Hua Yeow is also with the Singapore Institute for Neurotechnology and Advanced Robotics Center.

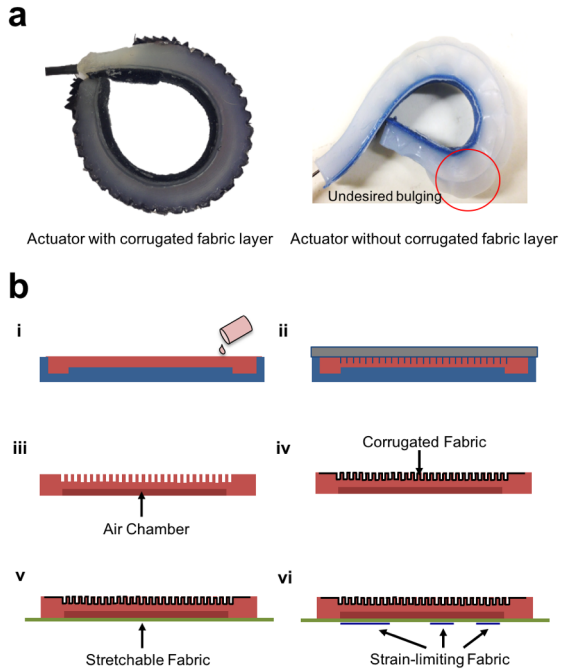


Fig. 1. a) Comparison of a soft pneumatic actuator with and without corrugated fabric layer. (b) Fabrication process of the actuator, i: Pour liquid elastomer (DragonSkin10, Smooth-On, Inc.) to the chamber mold, ii: Place the outer layer mold on top to create corrugated outer layer, iii: The ensemble is cured under 60°C, iv: A fabric was attached to the corrugated outer layer. v: Seal the bottom of the cured structure with a stretchable fabric, vi: Seal the bottom of the stretchable fabric with strain-limiting fabric at the locations corresponded to the finger joints.

II. SOFT PNEUMATIC ACTUATORS

A. Actuator Design and Fabrication

A number of research groups have developed soft pneumatic actuators such as PneuNets actuators [21] and fiber-reinforced actuators [22, 23] for the soft robotic glove application. Fiber reinforcement has been proved to be a robust method to constrain the undesired radial expansion which does not contribute to effective motion during pressurization. However, this method limits the bending capability of the actuators; as a result, higher pressure is needed to achieve desired bending.

In this paper, we developed a new type of soft fabric-regulated pneumatic actuators with a corrugated outer fabric layer which could minimize the excessive bulging and provide better bending capability compared to soft actuators used in previous studies [16, 24, 25]. This corrugated fabric layer allows a certain degree of initial radial expansion to initiate bending and then constrains any further radial expansion (Fig. 1a).

A two-part 3D-printed mold is required to fabricate the actuators. The lower-part mold (chamber mold) is used to create a pneumatic chamber inside the actuators, which will inflate upon pressurization, while the upper-part mold (outer layer mold) is used to impose the corrugated outer layer at the top of the actuators (Fig. 1b). The actuators can be fabricated and ready for use in less than one hour. Upon pressurization, the top surface of the actuators expands due to the inflation of the embedded pneumatic chamber. The strain-limiting fabric restricts the elongation at the bottom surface. This results in

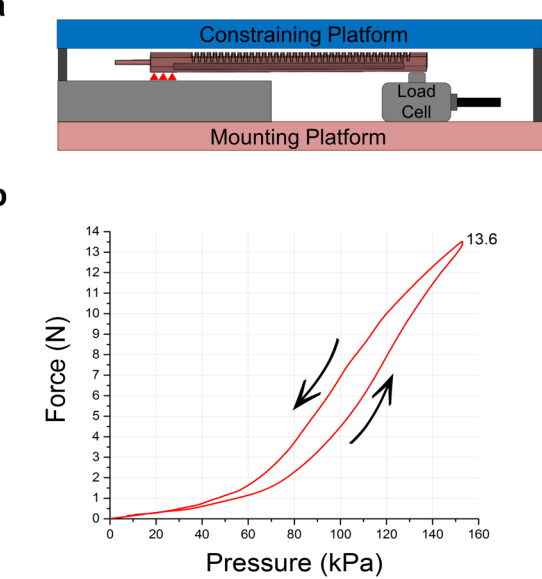


Fig. 2. a) Force measurement setup, b) Force – Pressure relationship of the actuator.

the bending of the actuators upon actuation. Combining both stretchable and strain-limiting fabrics at the bottom surface, the actuators can achieve bending and extending motions. The bending motion can support the flexion at the finger joints and the extending motion can offset the increased distance due to skin stretching when the finger is flexing.

B. Actuator Characterization

The initial tip force exerted by the actuator was measured over increasing pressures using a customized force measurement setup (Fig. 2a). The system consisted of a compression load cell (FC22, Measurement Specialties Inc, USA) and a mounting platform. The proximal end of the actuator was mounted on the platform and connected to the air source via a connecting tube. The distal end of the actuator was in contact with the load cell. A constraining platform was positioned on top of the actuator. During pressurization, the actuator flexed and started to contact with the constraining platform, which constrained the height and the curvature of the actuator (Fig. 2a). This force measurement setup was similar to the setup used in previous studies and the constraint was able to measure the initial tip force generated by the actuator regardless of the bending angle [14, 26].

The tip force increased with increased pressure (Fig. 2b). In the experiment, the maximum force and maximum actuation pressure tested for the actuators were 13.6N and 153kPa. According to a previous study which estimated that a minimum force of 8N was required to achieve a palmar grasp and manipulate most objects of daily living [14], the tip force of the actuator in this study was estimated to be sufficient to actuate the fingers and achieve a grasping action. Compared to the fiber-reinforced actuators which are made from Elastosil M4601 (Shore Hardness 28A) and operates at the pressure range of 275-375kPa [14], the actuators developed in this study were able to achieve similar force output at lower pressure, with a less stiff material (Shore Hardness 10A). With this advantage, the selection of the electro-pneumatic components, such as pump and valves, is less stringent.

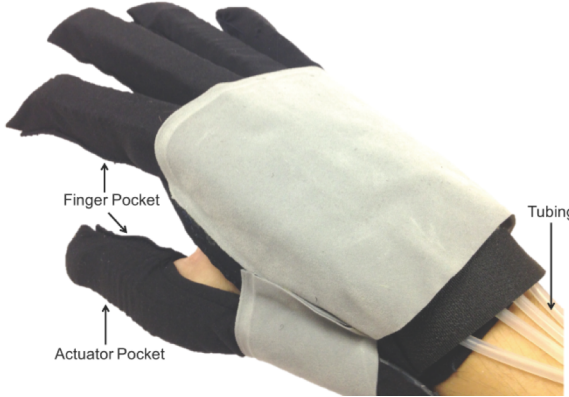


Fig. 3. A soft robotic glove prototype.

III. SOFT ROBOTIC GLOVE

A. Design Considerations

The overall structure of the device is a glove with five actuator-finger pockets attached on the dorsal side (Fig. 3). The glove serves as a compliant interfacing component to the human hand and provides minimal mechanical impedance to the finger motion when it is being worn. Open palm design is adopted for easy donning and doffing of the glove.

The soft actuators can be easily inserted into the actuator pockets. The actuator pockets are made from stretchable lycra fabrics, which serve as second constraining layers for the actuators. Each actuator is isolated with respect to the others, thus the assistance of each finger can be achieved independently, which allows execution of different grasp and release tasks. When the air pressure is removed from the actuators, the wearers can freely flex their fingers and grab real objects.

For the thumb actuator, the design at the top surface of the actuator is modified to support the opposition motion of the thumb, which includes bending of the interphalangeal (IP) and metacarpophalangeal (MCP) joints, extension in between the segments as well as bending and twisting around the carpo-metacarpal (CMC) joint (Fig. 4).

The total weight of the device is approximately 170g, which is much smaller than the typical design requirement of 450g for any device on the hand [27]. Additionally, as the actuators work under air pressure, inflation of the actuators does not add significant amount of extra weight to the hand.

B. Control System

An electro-pneumatic control system was assembled and integrated into a waist belt in order to allow isolated control of each actuator (Fig. 5). The control system consisted of voltage regulators and a microcontroller (Arduino Mega, Arduino). The pneumatic system consisted of air pressure sensors (MPX5500DP, Freescale, USA) for regulation of air pressure within each actuator, miniature solenoid valves (X-Valve, Parker, USA), and a miniature diaphragm pneumatic pump (D737-23-01, Parker, USA). The microcontroller regulated the measured air pressure (P) to track the desired air pressure (P_{ref}) and used pulse width modulation (PWM) to control the activation and deactivation of the valves and pump based on

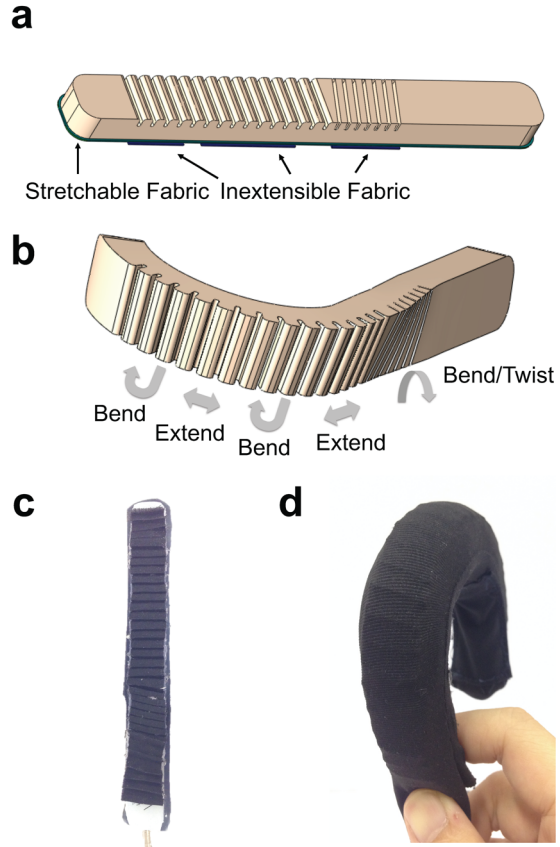


Fig. 4. a) Design of the thumb actuator with different types of fabrics. b) Combination of motions achieved under pressurization. c) Thumb actuators with a corrugated-fabric layer. d) Combination of motions achieved by the thumb actuator inside the actuator pocket.

the readings from the pressure sensors (Fig. 5c). The total weight of the waist belt was approximately 1.1kg.

IV. GLOVE EVALUATION

A. Kinematic Evaluation

An optical-based motion analysis system with eight cameras (VICON Motion System Ltd., UK) was used to capture the maximum range of motion of the glove-assisted finger of a healthy subject. Twelve reflective markers were attached to the glove according to the VICON Right Hand Model. The motion profiles of the index finger and thumb were tracked. The markers were attached to the index finger at locations corresponding to the fingertip, distal interphalangeal (DIP), proximal interphalangeal (PIP) and metacarpophalangeal (MCP) joints. For the thumb, the markers were attached to IP, MCP, and CMC joints. The actuators for the four fingers were pressurized at 120kPa and the thumb actuator was pressurized at 100kPa.

The trajectories of the markers were recorded by the cameras at a sampling rate of 100Hz. The kinematics data were averaged across three trials and analyzed using VICON BodyBuilder and VICON BodyLanguage (Vicon Motion System Ltd., UK) with customized code to calculate the range of motion of each joint (Table I).

For the index finger, the mean peak flexion angles for DIP, PIP and MCP were $46.4 \pm 9.9^\circ$, $84.3 \pm 6.8^\circ$, and $79.2 \pm 4.1^\circ$

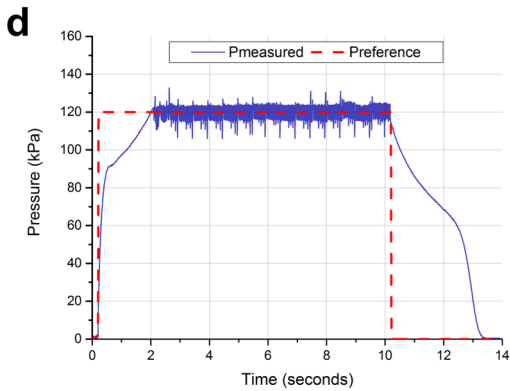
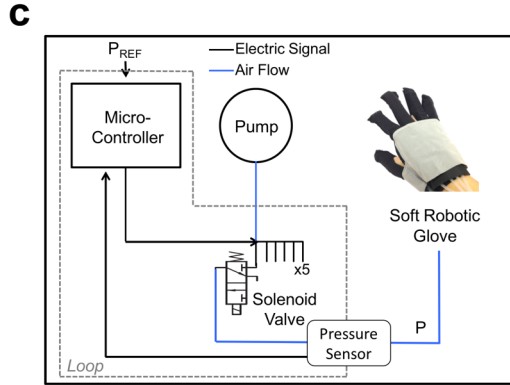
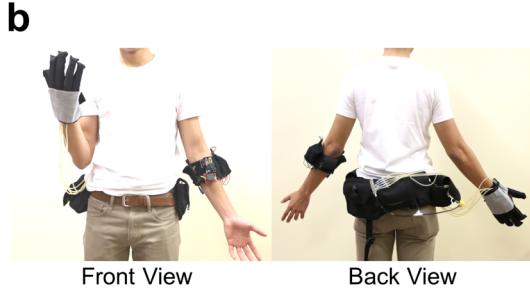
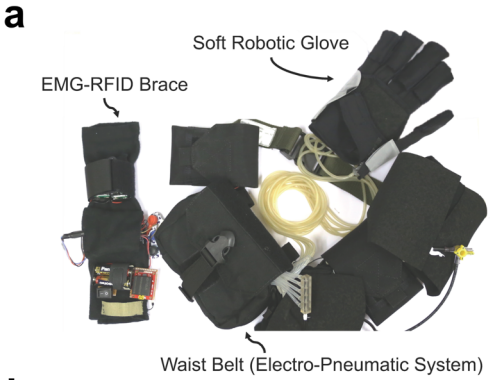


Fig. 5. a) Waist belt consists of electro-pneumatic components. b) Front and back view of an individual wearing the glove and waist belt. c) Schematic diagram of the control scheme for the soft robotic glove. d) The step response of the controller. PID control scheme was implemented on the microcontroller with a sampling frequency of 100Hz.

respectively (Fig. 6a). For the thumb, the mean peak flexion angles for IP, MP and CMC were $25.4 \pm 3.1^\circ$, $84.7 \pm 2.8^\circ$, and $62.9 \pm 2.4^\circ$ respectively. The glove-assisted thumb was able to touch the MCP joint crease of the little finger (Figure 6b), which corresponded to a Kapandji score of 9.



Fig. 6. a) Finger flexion, b) Thumb opposition achieved with the assistance of the soft robotic glove.

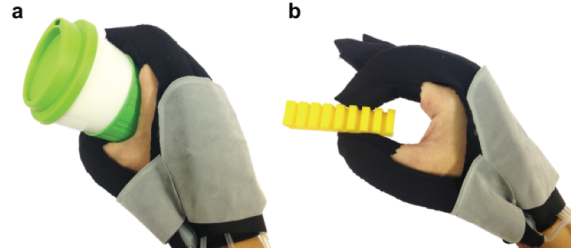


Fig. 7. a) Palmar grasp, b) Pincer grasp achieved with the assistance of the soft robotic glove

TABLE I. MAXIMUM RANGE OF MOTION

Finger	Joint	Max. Range of Motion ($^\circ$)
Index	DIP	46.4 ± 9.9
	PIP	84.3 ± 6.8
	MCP	79.2 ± 4.1
Thumb	IP	25.4 ± 3.1
	MP	84.7 ± 2.8
	CMC	62.9 ± 2.4

B. Kinetic Evaluation

Two manipulation tasks (palmar grasp and pincer grasp) were performed with the assistance of the soft robotic glove (Fig. 7). A 500g travel mug was used for palmar grasp and a 100g rectangular object was used for pincer grasp. Five flexible force sensors (Flexiforce A201, Tekscan Inc, USA) were slotted into the finger pockets. The force output at the finger tip during the tasks was measured and shown in Table 2.

TABLE II. FORCE OUTPUT

Action	Finger	Force (N)
Palmar Grasp	Thumb	0.52 ± 0.08
	Index	1.16 ± 0.26
	Middle	1.57 ± 0.14
	Ring	0.81 ± 0.09
	Small	0.76 ± 0.09
Pincer Grasp	Thumb	0.42 ± 0.09
	Index	1.24 ± 0.13

V. EMG-RFID CONTROL STRATEGY

A. EMG-RFID Brace

A customized EMG-RFID brace is used to detect the user intention by measuring the electrical activity of two muscles on the forearm. The brace consists of two sets of low-cost muscle sensors (Advancer Technologies, USA) and a RFID sensor (ID-12LA, ID-innovations, Australia). The RFID tags

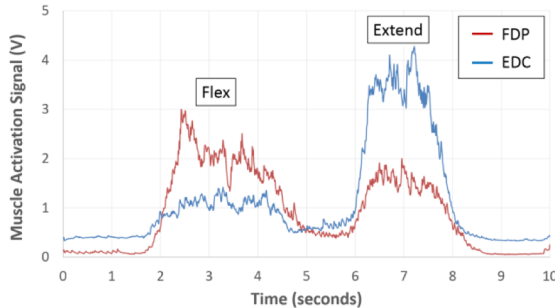


Fig. 8. EMG signals during maximum voluntary contractions.

serve as non-physical switches to activate different pre-selected groups of actuators that corresponded to different tasks. This approach is more intuitive than the mechanical switches and could possibly reduce the time required to complete different manipulation tasks. The weight of the EMG-RFID brace was 260g.

B. Maximum Voluntary Contraction

The sEMG electrodes were attached to the finger flexor muscles (flexor digitorum profundus, FDP) and finger extensor muscles (extensor digitorum communis, EDC) of a healthy participant. The participant was instructed to perform maximal voluntary muscle contractions (MVC) while flexing and extending the fingers. The values were shown in Figure 8.

C. User Intent Detection

Figure 9 demonstrates different possible EMG-RFID control strategies. In this work, we explore one of the strategies, which is using the unimpaired hand to control the activation of the soft robotic glove on the impaired hand. This strategy is suitable for those with extremely weak arm and hand strength, for example, an individual with brachial plexus injury. This group of users have little to no residual muscle activation which can be detected by the sEMG electrodes on the impaired forearm.

An open-loop sEMG logic (similar to the approach presented in [20]) is adopted to detect the user intent. The control of the soft robotic glove can be achieved by monitoring the state of the two muscle signals (FDP and EDC) to three predefined conditions: a) ‘activate’, b) ‘hold’, and c) ‘release’. The ‘activate’ condition is met when the muscle signal from the FDP muscle exceeds the flexor threshold. In this condition, the pre-selected group of actuators will be pressurized, flexing the fingers. The ‘release’ condition is met when the muscle signal from the EDC muscle exceeds the extensor threshold. In this condition, the actuators will be depressurized and the fingers will be returned to the extended position. The ‘hold’ condition is activated when both the ‘activate’ and ‘release’ conditions are not met. The actuators will maintain the present condition until the next condition is met. The threshold can be further adjusted based on the pathology and residual muscle activity of the user.

In this work, two RFID tags were attached to the objects and served as the switches for two tasks (palmar grasp and pincer grasp). Figure 10a and 10b show that the participant was able to perform a palmar grasp by scanning the tags on the travel mug using the RFID sensor while activating the ‘activate’ condition. Similarly, the healthy participant was

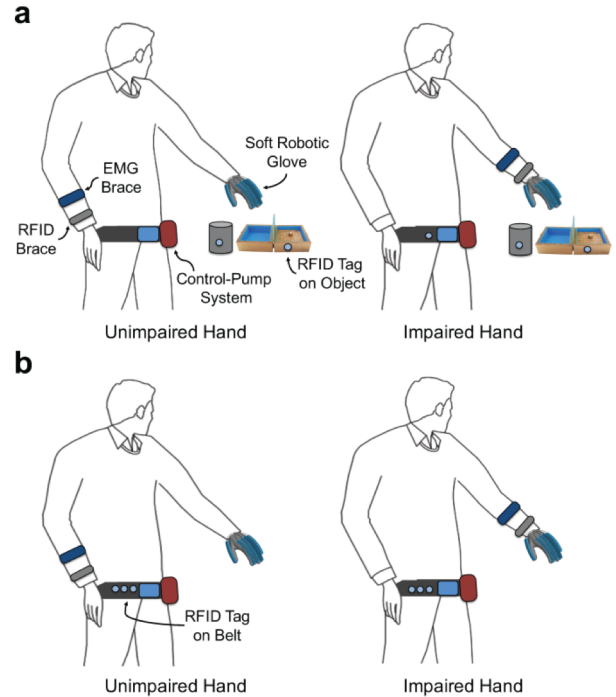


Fig. 9. EMG-RFID control strategies. a) RFID tags attached on the objects. b) RFID tags attached on the belt. The user can control the soft robotic glove using unimpaired or impaired hand.

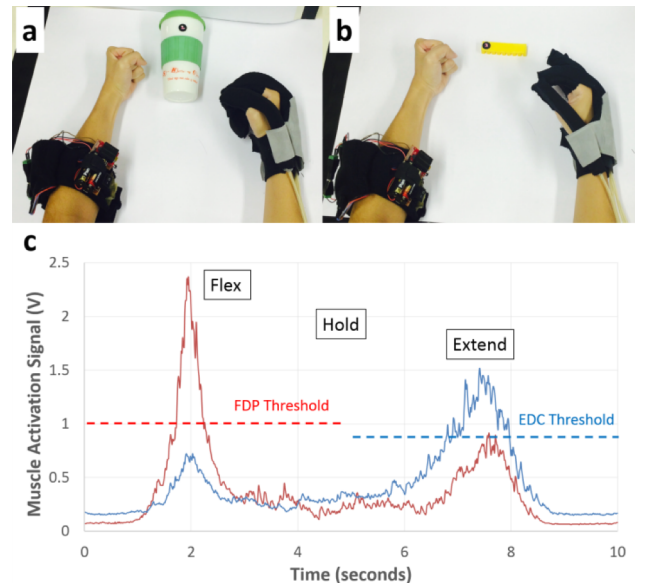


Fig. 10. a) Participant performing palmar grasp with the unimpaired hand. b) Participant performing pincer grasp with the unimpaired hand. c) The EMG signals collected from FDP and EDC muscles during the palmar grasp.

able to perform a pincer grasp by scanning the tags on the rectangular object while activating the ‘activate’ condition. When ‘release’ condition was met, the objects were released from the hand. Figure 10c shows the muscle signals collected from FDP and EDC muscles during the palmar grasp, alongside their corresponding thresholds (which was 30% of FDP-MVC and 20% of EDC-MVC for the particular participant).

VI. CONCLUSION

In this paper, we presented a soft robotic glove that is able to provide assistance to individuals with functional grasp pathologies during activities of daily living. The glove utilizes soft fabric-regulated pneumatic actuators that are low-profile as they are able to achieve similar force output at lower pressure, with a less stiff material, as compared to previously developed soft actuators. A corrugated-fabric layer is imposed on the outer surface of the actuators, which constrains the undesired radial expansion effectively. Combining different types of textiles at the bottom surface of the actuators, the actuators can generate complex motions to support full hand range of motion.

Experiments were conducted to characterize the actuators in terms of the force output and input pressure relationship. The soft robotic glove was evaluated in terms of the kinematic profile of the assisted finger and thumb as well as the fingertip force during palmar and pincer grasps. Different EMG-RFID control strategies were proposed and preliminary results demonstrated that a healthy participant was able to control the soft robotic glove and achieve palmar and pincer grasps using a combined EMG-RFID control strategy. Further work is planned to conduct a larger study with patients with functional grasp pathologies in order to improve the actuator and glove design. Additionally, more complicated and practical usages of the EMG-RFID control strategies, such as grasping cylindrical objects with different diameters, will be explored. Finally, a bi-directional soft robotic glove that is capable to provide active flexion and active extension will be designed to cater for a larger patient population.

ACKNOWLEDGEMENT

The authors would like to thank NUS Graduate School for Integrative Sciences and Engineering for providing scholarship support to the first author of this paper.

REFERENCES

- [1] W. Muellbacher, C. Richards, U. Ziemann, G. Wittenberg, D. Weltz, B. Boroojerdi, *et al.*, "Improving hand function in chronic stroke," *Arch Neurol*, vol. 59, pp. 1278-82, 2002.
- [2] M. B. Wagner, P. J. Vignos, Jr., C. Carlozzi, and A. L. Hull, "Assessment of hand function in Duchenne muscular dystrophy," *Arch Phys Med Rehabil*, vol. 74, pp. 801-4, 1993.
- [3] G. J. Snoek, M. J. Ijzerman, H. J. Hermens, D. Maxwell, and F. Biering-Sorensen, "Survey of the needs of patients with spinal cord injury: impact and priority for improvement in hand function in tetraplegics," *Spinal Cord*, vol. 42, pp. 526-532.
- [4] L. Rosenstein, A. L. Ridgel, A. Thota, B. Samame, and J. L. Alberts, "Effects of combined robotic therapy and repetitive-task practice on upper-extremity function in a patient with chronic stroke," *Am J Occup Ther*, vol. 62, pp. 28-35, 2008.
- [5] P. Maciejasz, J. Eschweiler, K. Gerlach-Hahn, A. Jansen-Troy, and S. Leonhardt, "A survey on robotic devices for upper limb rehabilitation," *Journal of NeuroEngineering and Rehabilitation*, vol. 11, p. 3, 2014.
- [6] M. F. Rotella, K. E. Reuther, C. L. Hofmann, E. B. Hage, and B. F. BuSha, "An orthotic hand-assistive exoskeleton for actuated pinch and grasp," in *IEEE 35th Annual Northeast Bioeng. Conf.*, 2009, pp. 1-2.
- [7] L. A. Martinez, O. O. Olaloye, M. V. Talarico, S. M. Shah, R. J. Arends, and B. F. BuSha, "A power-assisted exoskeleton optimized for pinching and grasping motions," in *IEEE 36th Annual Northeast Bioengineering Conference*, 2010, pp. 1-2.
- [8] T. T. Worsnopp, M. A. Peshkin, J. E. Colgate, and D. G. Kamper, "An Actuated Finger Exoskeleton for Hand Rehabilitation Following Stroke," in *IEEE Inter. Conf. on Rehabilitation Robotics (ICORR)*, 2007, pp. 896-901.
- [9] M. Nilsson, J. Ingvast, J. Wikander, and H. von Holst, "The Soft Extra Muscle system for improving the grasping capability in neurological rehabilitation," in *IEEE EMBS Conf. on Biomedical Engineering and Sciences (IECBES)*, 2012, pp. 412-417.
- [10] V. Varalta, A. Picelli, C. Fonte, G. Montemezzi, E. La Marchina, and N. Smania, "Effects of contralesional robot-assisted hand training in patients with unilateral spatial neglect following stroke: a case series study," *Journal of NeuroEngineering and Rehabilitation*, vol. 11, p. 160, 2014.
- [11] L. Sangwook, K. A. Landers, and P. Hyung-Soon, "Development of a Biomimetic Hand Exotendon Device (BiomHED) for Restoration of Functional Hand Movement Post-Stroke," *IEEE Transactions on Neural Systems and Rehabilitation Engineering*, vol. 22, pp. 886-898, 2014.
- [12] R. V. Martinez, J. L. Branch, C. R. Fish, L. Jin, R. F. Shepherd, R. M. D. Nunes, *et al.*, "Robotic Tentacles with Three-Dimensional Mobility Based on Flexible Elastomers," *Advanced Materials*, vol. 25, pp. 205-212, 2013.
- [13] D. Rus and M. T. Tolley, "Design, fabrication and control of soft robots," *Nature*, vol. 521, pp. 467-475, 2015.
- [14] P. Polygerinos, Z. Wang, K. C. Galloway, R. J. Wood, and C. J. Walsh, "Soft robotic glove for combined assistance and at-home rehabilitation," *Robotics and Autonomous Systems*.
- [15] P. Polygerinos, K. C. Galloway, E. Savage, M. Herman, K. O. Donnell, and C. J. Walsh, "Soft robotic glove for hand rehabilitation and task specific training," in *IEEE Inter. Conf. on Robotics and Automation (ICRA)*, 2015, pp. 2913-2919.
- [16] H. K. Yap, J. H. Lim, F. Nasrallah, J. C. H. Goh, and R. C.-H. Yeow, "A Soft Exoskeleton for Hand Assistive and Rehabilitation Application using Pneumatic Actuators with Variable Stiffness," in *IEEE Inter. Conf. on Robotics and Automation (ICRA)*, 2015, pp. 4967-4972.
- [17] H. K. Yap, J. H. Lim, F. Nasrallah, F.-Z. Low, J. C. H. Goh, and R. C.-H. Yeow, "MRC-Glove: A fMRI Compatible Soft Robotic Glove for Hand Rehabilitation Application," in *IEEE Inter. Conf. on Rehabilitation Robotics (ICORR)*, 2015, pp. 735-740.
- [18] M. J. Scherer, C. Sax, A. Vanbiervliet, L. A. Cushman, and J. V. Scherer, "Predictors of assistive technology use: the importance of personal and psychosocial factors," *Disabil Rehabil*, vol. 27, pp. 1321-31, 2005.
- [19] M. Scherer, J. Jutai, M. Fuhrer, L. Demers, and F. Deruyter, "A framework for modelling the selection of assistive technology devices (ATDs)," *Disabil Rehabil Assist Technol*, vol. 2, pp. 1-8, Jan 2007.
- [20] P. Polygerinos, K. C. Galloway, S. Sanan, M. Herman, and C. J. Walsh, "EMG Controlled Soft Robotic Glove for Assistance During Activities of Daily Living," in *IEEE Inter. Conf. on Rehabilitation Robotics (ICORR)*, 2015, pp. 55-60.
- [21] B. Mosadegh, P. Polygerinos, C. Kepplinger, S. Wennstedt, R. F. Shepherd, U. Gupta, *et al.*, "Pneumatic Networks for Soft Robotics that Actuate Rapidly," *Advanced Functional Materials*, vol. 24, pp. 2163-2170, 2014.
- [22] K. C. Galloway, P. Polygerinos, C. J. Walsh, and R. J. Wood, "Mechanically programmable bend radius for fiber-reinforced soft actuators," in *Inter. Conf. on Advanced Robotics (ICAR)*, 2013, pp. 1-6.
- [23] P. Polygerinos, Z. Wang, J. T. B. Overvelde, K. C. Galloway, R. J. Wood, K. Bertoldi, *et al.*, "Modeling of Soft Fiber-Reinforced Bending Actuators," *IEEE Trans. on Robotics*, pp. 1-12, 2015.
- [24] Y. Elsayed, A. Vincensi, C. Lekakou, T. Geng, C. M. Saaj, T. Ranzani, *et al.*, "Finite Element Analysis and Design Optimization of a Pneumatically Actuating Silicone Module for Robotic Surgery Applications," *Soft Robotics*, vol. 1, pp. 255-262, 2014.
- [25] H. K. Yap, J. C. H. Goh, and C. H. Yeow, "Design and Characterization of Soft Actuator for Hand Rehabilitation Application," in *6th Europ. Conf. of the International Federation for Medical and Biological Engineering*, 2015, pp. 367-370.
- [26] D. Sasaki, T. Noritsugu, M. Takaiwa, and H. Yamamoto, "Wearable power assist device for hand grasping using pneumatic artificial rubber muscle," in *IEEE Inter. Workshop on Robot and Human Interactive Communication*, 2004, pp. 655-660.
- [27] P. M. Aubin, H. Sallum, C. Walsh, L. Stirling, and A. Correia, "A pediatric robotic thumb exoskeleton for at-home rehabilitation: the Isolated Orthosis for Thumb Actuation (IOTA)," *IEEE International Conference on Rehabilitation Robotics (ICORR)*, vol. 2013, p. 6650500, Jun 2013.